

# Second Comparative Solution Project: A Three-Phase Coning Study

H.G. Weinstein, SPE, H.J. Gruy & Assocs. Inc.  
J.E. Chappellear, SPE, Shell Development Co.  
J.S. Nolen, SPE, J.S. Nolen & Associates

SPE 10489

**Summary.** Eleven companies participated in the Second Comparative Solution Project. The problem to be solved is a three-phase coning problem that can be described as a radial cross section with one central producing well. The oil and water densities are nearly equal, so the oil/water capillary transition zone extends high up into the oil column. Wide variations in rates occur, and the solution GOR is unusually high for oil with such high density. These problem characteristics make the problem difficult to solve, thus increasing its value as a test of simulation techniques. Various aspects of the numerical solutions obtained are compared in this paper. In general, the solutions agree reasonably well.

## Introduction

The previous effort in this series<sup>1</sup> generated considerable interest. On request, on April 30, 1981, Aziz Odeh presented the paper for a second time to a full house of the London Petroleum Section of SPE. The interest in continuing a project such as this is great—both in the U.S. and abroad. Following his London success, Aziz Odeh wrote in a letter to SPE, "Extension of the cooperative effort started with this publication to cover more complex models and problems would be very beneficial to the industry. I recommend that the SPE undertake such an endeavor. I believe the industry will welcome such a project." During the organization of the 1982 SPE Symposium on Reservoir Simulation, the program chairman, Khalid Aziz, therefore suggested that we organize a comparison of results on another test problem.

Because the previous problem had been a field-scale simulation, it was suggested that a coning study might be of interest. A problem drawn from an actual field case was simplified somewhat to provide a challenging test problem. It is a single-well radial cross section that involves gas and water coning as well as gas repressuring. It is a difficult problem that provides a good test of the stability and convergence behavior of any simulator.

Invitations were mailed to a number of oil companies and consulting organizations. Eleven companies chose to participate in the project (Table 1). The organizers tried to invite every company that had a distinct simulation capability. Doubtless, some were inadvertently omitted, and we apologize to such groups.

We feel that the numerical solutions obtained agree surprisingly well, considering the diversity of discretization and solution techniques used. Whether the consensus is actually close to the mathematical solution is, of course, still an open question. The paper presents the text of the problem, a comparison of results in graphical and tabular form, and a brief description of each model. We have

included a display of data concerning simulator performance (e.g., number of timesteps, number of Newtonian iterations, and timing). Calculations were performed on a number of different computers. Because the problem is small, it is difficult to draw any general conclusions from the data; in this paper, we point out a few ideas that have occurred to us.

As remarked by some participants, the problem is rather artificial in that it involves rate variations that would not be likely to occur in practice. Furthermore, the solution GOR is unusually high for oil with such a high density. Both of these characteristics, however, make the problem more difficult to solve, increasing its value as a test of simulation techniques.

## Description of the Simulators

**ARCO Oil and Gas Co.** ARCO's two coning simulators are implicit, three-phase, black-oil simulators. The numerical formulation in both versions is a linearized semi-implicit scheme with upstream weighting for phase mobilities. Within a timestep, only the nonlinear accumulation term is updated if necessary. The algebraic equations are solved directly.

One version treats the wells as distributed sources and sinks. Phase and layer production rate allocation are based on the phase mobility of each layer. The D4 reordering scheme is used to improve efficiency.<sup>2</sup> Three-phase relative permeabilities are calculated by Stone's first method.<sup>3</sup>

The second version strongly couples a well equation with the reservoir equations and solves simultaneously for the reservoir variables, as well as the well rate or bottomhole pressure (BHP). Pressure gradient in the wellbore is assumed hydrostatic. Standard ordering of gridblocks is used for solution of linear equations. Three-phase relative permeabilities are calculated by Stone's second method.<sup>4</sup>

**TABLE 1—COMPANIES PARTICIPATING IN SPE COMPARATIVE SOLUTION PROJECT**

ARCO Oil and Gas Co. P.O. Box 2819 Dallas, TX 75221	Intercomp Suite 1100 10333 Richmond Houston, TX 77042
Chevron Oil Field Research Co. P.O. Box 446 La Habra, CA 90631	McCord-Lewis Energy Services P.O. Box 45307 Dallas, TX 75245
D&S Research and Development Ltd. 200 Pembina Place 1035 7th Ave. S.W. Calgary, Alta., Canada T2P 3E9	J.S. Nolen & Assocs. Suite 560 16225 Park 10 Place Houston, TX 77084
Franlab Consultant, S.A. Petroleum Engineers B.P. No. 14 06561 Valbonne Cedex, France	Scientific Software Corp. 18th Floor First of Denver Plaza Building 633 17th Street Denver, CO 80202
Gulf Research and Development Co. P.O. Drawer 2038 Pittsburgh, PA 15230	Shell Development Co. P.O. Box 481 Houston, TX 77001
Harwell Operations Research Group Computer Science and Systems Div. Building 8.19 AERE Harwell, Oxfordshire, England	

**TABLE 2—RESERVOIR DESCRIPTION**

Layer	Thickness (ft)	$k_x$ (md)	$k_z$ (md)	Porosity*
1	20	35.000	3.500	0.087
2	15	47.500	4.750	0.097
3	26	148.000	14.800	0.111
4	15	202.000	20.200	0.160
5	16	90.000	9.000	0.130
6	14	418.500	41.850	0.170
7	8	775.000	77.500	0.170
8	8	60.000	6.000	0.080
9	18	682.000	68.200	0.140
10	12	472.000	47.200	0.130
11	19	125.000	12.500	0.120
12	18	300.000	30.000	0.105
13	20	137.500	13.750	0.120
14	50	191.000	19.100	0.116
15	100	350.000	35.000	0.157

\*Porosity is at reference pressure (3,600 psi).

The test problem was solved with both simulators, but ARCO believes the second model to be more accurate. The results reported here were calculated by the second model.

**Chevron Oil Field Research Co.** The coning option of Chevron's general-purpose black-oil reservoir simulator (CRS-3D) was used. For this option, the program performs a fully implicit, simultaneous calculation of pressure, saturation, and wellbore BHP. Nonlinear conservation equations for oil, gas, and water are obtained for each cell by use of a finite-difference discretization. These equations, together with the well-constraint equation, are linearized and iterated to convergence by the Newton-Raphson method. Linear equations are solved with sparse Gaussian elimination and D4 ordering.

Timesteps are automatically selected by a comparison of maximum values of calculated pressure and saturation

changes for the current timestep to user-specified quantities. The next timestep is estimated by the multiplication of the current timestep by the most restrictive ratio of user-specified value to maximum calculated value for the current timestep. A maximum timestep value of 11 days was used for this run. When the Newton-Raphson method does not converge after 10 iterations, the timestep is halved. This is considered to be a "backup."

**D&S Research and Development Ltd.** The D&S simulator is a fully implicit, three-dimensional (3D), three-phase program that solves simultaneously for all unknowns.

At each iteration in each timestep, the coefficients of the matrix are obtained by the Newton-Raphson method. Variable substitution is used to reduce the number of unknowns and to handle the reappearance/disappearance of the phases. The system of linear equations is then solved simultaneously with an iterative method that is based on the ITD4MIN procedure.<sup>5</sup> In large-scale simulations, most of the computing time is spent in solution of the matrix of coefficients rather than in the generation of the coefficients. Use of the fully implicit coefficients ensures maximum stability, and the use of simultaneous solution avoids problems of decoupling the equations. The iterative method employed significantly reduces the computing time for the solution of the system of linear equations, and this, for large problems, more than outweighs the additional time spent in the fully implicit simultaneous-solution approach.

Stone's second relative-permeability model is used with single-point upstream weighting.

**Franlab Consultant, S.A.** The Franlab simulator is a two-dimensional (2D), three-phase program that solves simultaneously for  $p_o$ ,  $S_w$ , and  $S_g$ .<sup>6</sup> Semi-implicit approximations are used for relative permeability and capil-

TABLE 3—BASIC DATA

<u>Geometry</u>	
Radial extent, ft	2,050
Wellbore radius, ft	0.25
Radial position of first block center, ft	0.84
Number of radial blocks	10
Radial block boundaries, ft	0.25, 2.00, 4.32, 9.33, 20.17, 43.56, 94.11, 203.32, 439.24, 948.92, and 2,050.00
Number of vertical layers	15
Dip angle, degrees	0
Depth to top of formation, ft	9,000
<u>Rock and Fluid Data</u>	
Pore compressibility, $\text{psi}^{-1}$	$4 \times 10^{-6}$
Water compressibility, $\text{psi}^{-1}$	$3 \times 10^{-6}$
Oil compressibility for undersaturated oil, $\text{psi}^{-1}$	$1 \times 10^{-5}$
Oil viscosity compressibility for undersaturated oil, $\text{psi}^{-1}$	0
Stock-tank oil density, lbm/cu ft	45.0
Stock-tank water density, lbm/cu ft	63.02
Standard-condition gas density, lbm/cu ft	0.0702
<u>Initial Conditions</u>	
Depth of gas/oil contact, ft	9,035
Oil pressure at gas/oil contact, psi	3,600
Capillary pressure at gas/oil contact, psi	0
Depth of water/oil contact, ft	9,209
Capillary pressure at water/oil contact, psi	0
<u>Well Data</u>	
Completed in blocks*	(1,7) (1,8)
Permeability/thickness, md-ft	6,200 480
Skin	0 0
Minimum BHFP, psi	3,000
Pump depth, ft	9,110
<u>Production Schedule</u>	
Time Period (days)	Oil Production Rate,** (STB/D)
1 to 10	1,000
10 to 50	100
50 to 720	1,000
720 to 900	100

\*The well is located at the inner boundary of each gridblock.

\*\*The production schedule is to be maintained until the BHFP is equal to the constraint value.

lary pressure. Nonlinear terms are not iterated. The linearized finite-difference equations are solved by Gaussian elimination with conventional ordering.

The capillary end effect is taken into account in the boundary conditions for the well. BHP's are calculated implicitly with an iterative procedure.

Oil relative permeabilities are calculated by a procedure that linearly interpolates between water/oil and gas/oil curves on the basis of a ternary diagram.

**Gulf Research and Development Co.** The Gulf black-oil coning model employs standard point-centered spatial differencing and fully implicit backward time differencing. The well equations are fully coupled in that the wellbore pressure at each producing node is an unknown. The nonlinear equations are solved by a modified Newton method. For this problem, a direct solver was used to solve the linear equations.

The formulation incorporates capillary end effects. The end effect is based on the assumption that the oil pres-

sure is continuous from the reservoir to the wellbore, water is not produced until water saturation reaches the zero of the imbibition capillary-pressure curve, and gas is not produced until gas saturation reaches critical saturation. Once these saturations are reached, they remain at these values. Because no imbibition curve data were provided, the zero of the imbibition curve was assumed to occur at  $S_w = 0.8$ .

Because the finite-difference method is point-centered, different mesh points than those prescribed in the original data were used. In the  $r$  direction, the mesh, given as distance from the origin in feet, is

0.25 ( $r_w$ ), 2.00, 4.32, 9.33, 20.17, 43.56, 94.11, 203.32, 439.24, 948.92, and 2,050.00.

In meters:

0.08, 0.61, 1.32, 2.84, 6.15, 13.28, 28.68, 61.97, 133.88, 289.23, and 624.84.

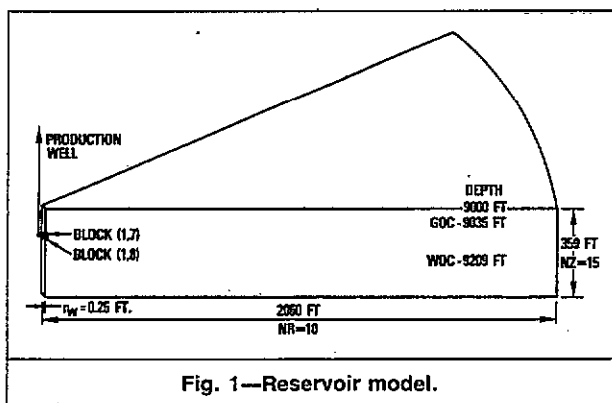


Fig. 1—Reservoir model.

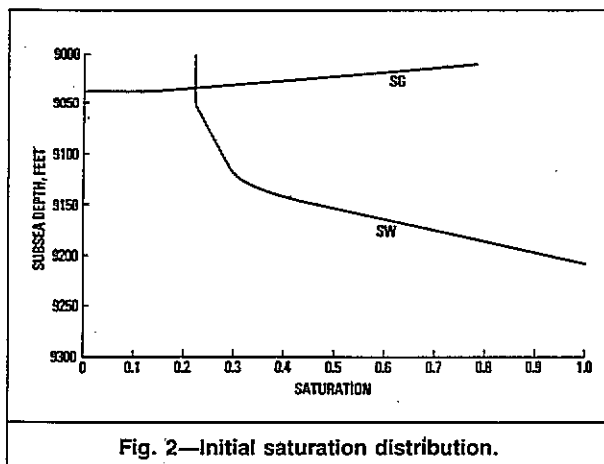


Fig. 2—Initial saturation distribution.

TABLE 4—SATURATION FUNCTIONS

$S_w$	Water/Oil Functions		$P_{cow}$
	$k_{rw}$	$k_{row}$	
0.22	0.0	1.0	7.0
0.30	0.07	0.4000	4.0
0.40	0.15	0.1250	3.0
0.50	0.24	0.0649	2.5
0.60	0.33	0.0048	2.0
0.80	0.65	0.0	1.0
0.90	0.83	0.0	0.5
1.00	1.0	0.0	0.0

$S_g$	Gas/Oil Functions		$P_{cgo}$
	$k_{rg}$	$k_{rog}$	
0.0	0.0	1.0	0.0
0.04	0.0	0.60	0.2
0.10	0.0220	0.33	0.5
0.20	0.1000	0.10	1.0
0.30	0.2400	0.02	1.5
0.40	0.3400	0.0	2.0
0.50	0.4200	0.0	2.5
0.60	0.5000	0.0	3.0
0.70	0.8125	0.0	3.5
0.78	1.0	0.0	3.9

In the  $z$  direction, the mesh, given as depth from the surface in feet, is

9,012.50, 9027.50, 9,042.50, 9,055.50, 9,066.50, 9,085.50, 9,098.50, 9,113.50, 9,114.50, 9,129.50, 9,150.50, 9,153.50, 9,188.50, 9,189.50, 9,228.50, and 9,289.50.

In meters:

2747.01, 2751.58, 2756.15, 2760.12, 2763.47, 2769.26, 2773.22, 2777.79, 2778.10, 2782.67, 2789.07, 2789.99, 2800.65, 2800.96, 2812.85, and 2831.44.

In addition, two other points in the  $z$  direction at depths of 8,987.50 and 9,428.50 ft [2739.4 and 2873.8 m] were added. Fully sealing faults were placed at 9,000.0 and 9,359.0 ft [2743.2 and 2852.6 m]. The purpose of these points and the faults was to model a block-centered system better. As a result, 198 mesh points were used vs. the 150 cells in the problem statement. Oil relative permeabilities were calculated according to the Dietrich and Bondor technique for Stone's second method.<sup>7</sup> (For this problem, the Dietrich and Bondor modification is identical to Stone's method.)

**Harwell.** The test problem was solved with PORES, a general-purpose implicit, three-phase, 3D black-oil reservoir simulator.<sup>8</sup> Efficiency is achieved when the coupled equations are solved by a new sequential method that automatically ensures material balance. This method also conserves material and uses a truncated conjugate gradient technique to accelerate convergence. Simultaneous and direct solution options are also provided. PORES contains an extensive well model that is numerically stable, meets production targets precisely, and apportions flows accurately to individual layers of the reservoir model. The user can specify whether free gas is allowed to dissolve in oil during repressurization. Relative permeabilities may be calculated with either single-point or two-point upstream weighting. Three-phase oil relative permeabilities are calculated with either Stone's second method or an unpublished method developed at Harwell.

The test problem was solved with single-point upstream weighting with both relative permeability methods. Runs with both repressurization options gave equivalent results. The results reported used the "no-resolution" option and Stone's formula. The CPU times quoted were obtained with the iterative matrix solver, which was significantly faster than the direct solver in this case.

**Intercomp.** The test problem was solved with the implicit-flow model, which simulates one-, two-, or three-dimensional isothermal flow of three phases in Cartesian or cylindrical coordinates.<sup>9</sup>

The model treats two hydrocarbon components, is fully implicit for reliability (stability) with one exception, and accounts for the presence of vaporized oil in the gas phase ( $r_s$ ) in addition to dissolved gas ( $R_s$ ). It therefore simulates gas condensate reservoirs that do not require fully compositional (multicomponent) PVT treatment. The one exception to the fully implicit treatment is a semi-implicit treatment of the allocation of a well's total rate among its several completed layers.

Linearization of the finite-difference equations gives three difference equations (for each gridblock) in the six dependent variables  $\delta S_w$ ,  $\delta S_o$ ,  $\delta S_g$ ,  $\delta R_s$ ,  $\delta r_s$ , and  $\delta p$ . If the gridblock is two-phase water/oil, then  $\delta S_g$  and  $\delta r_s$  disappear from the list of six unknowns and the saturation constraint allows elimination of  $\delta S_w$  or  $\delta S_o$ . If the block is two-phase gas/water, then  $\delta S_o$  and  $\delta R_s$  disappear and the saturation constraint allows elimination of  $\delta S_w$  or  $\delta S_g$ . Thus in any case, the linearized primary

TABLE 5—PVT PROPERTIES

Pressure (psia)	Saturated Oil				Water			Gas		
	$B_o$ (RB/STB)	Density (lbm/cu ft)	Viscosity (cp)	Solution GOR (scf/STB)	$B_w$ (RB/STB)	Density (lbm/cu ft)	Viscosity (cp)	$B_g$ (Mcf/STB)	Density (lbm/cu ft)	Viscosity (cp)
400	1.0120	46.497	1.17	165	1.01303	62.212	0.96	5.90	2.119	0.0130
800	1.0255	48.100	1.14	335	1.01182	62.286	0.96	2.95	4.238	0.0135
1,200	1.0380	49.372	1.11	500	1.01061	62.360	0.96	1.96	6.397	0.0140
1,600	1.0510	50.726	1.08	665	1.00940	62.436	0.96	1.47	8.506	0.0145
2,000	1.0630	52.072	1.06	828	1.00820	62.510	0.96	1.18	10.596	0.0150
2,400	1.0750	53.318	1.03	985	1.00700	62.585	0.96	0.98	12.758	0.0155
2,800	1.0870	54.399	1.00	1,130	1.00580	62.659	0.96	0.84	14.885	0.0160
3,200	1.0985	55.424	0.98	1,270	1.00460	62.734	0.96	0.74	16.896	0.0165
3,600	1.1100	56.203	0.95	1,390	1.00341	62.808	0.96	0.65	19.236	0.0170
4,000	1.1200	56.930	0.94	1,500	1.00222	62.883	0.96	0.59	21.192	0.0175
4,400	1.1300	57.534	0.92	1,600	1.00103	62.958	0.96	0.54	23.154	0.0180
4,800	1.1400	57.864	0.91	1,676	0.99985	63.032	0.96	0.49	25.517	0.0185
5,200	1.1480	58.267	0.90	1,750	0.99866	63.107	0.96	0.45	27.785	0.0190
5,600	1.1550	58.564	0.89	1,810	0.99749	63.181	0.96	0.42	29.769	0.0195

equations become three simultaneous equations in three unknowns that are solved by D4 direct solution or by an iterative method.

Relative permeabilities are calculated by a normalized variation of Stone's second method. (This variation is identical to Stone's method for this problem.) Single-point upstream weighting of relative permeabilities is used.

**McCord-Lewis Energy Services.** This simulator is a general-purpose 2D model that employs an FVF PVT description with a variable saturation pressure feature. The matrix grid can be located in the vertical or horizontal plane. Radial segments may be used on one axis in either mode of operation.

In the vertical mode, the model can be applied to the study of individual well problems. Its ability to describe several completion intervals in a single well lends itself to detailed coning calculations, special completion techniques, and the solution of other well problems. Relative-permeability approximations are semi-implicit (extrapolated over the timestep), and finite-difference equations are solved sequentially. In other words, the three equations for each gridblock are combined into a single pres-

sure equation, and then each of the three-phase saturations is calculated from a semi-implicit equation with known pressures. The entire sequence can be repeated with updated pressures and saturations.

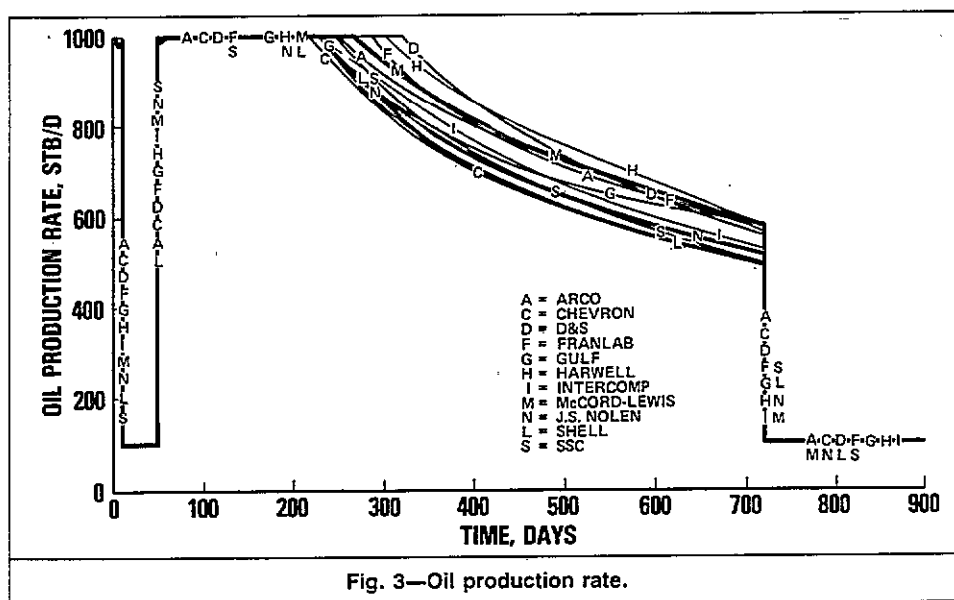
Oil relative permeabilities are calculated according to Stone's first method. The finite-difference equations are solved by Gaussian elimination with conventional ordering.

**J.S. Nolen and Assocs.** The test problem was solved with the vectorized implicit program (VIP), a general-purpose, 3D, three-phase black-oil simulator.<sup>10,11</sup> Because either rectangular or cylindrical grid networks can be used, VIP efficiently solves both single-well and field-scale production problems.

VIP is fully implicit in saturations and bubblepoints and uses a modified Newton-Raphson iteration to solve simultaneously for three unknowns per gridblock. [Optional finite-difference formulations include implicit pressure/explicit saturation (IMPES) and an implicit water/oil formulation that solves for two unknowns per gridblock.] BHP is iterated to the new time level.

TABLE 6—COMPARISON OF CALCULATED RESULTS

Company	Initial Fluids in Place			Time on Decline (days)	Timesteps	Timestep Cuts	Nonlinear Updates	Matrix Solution	Computer	CPU Time (seconds)	Comments
	Oil (10 <sup>6</sup> STB)	Water (10 <sup>6</sup> STB)	Gas (10 <sup>6</sup> scf)								
ARCO	28.80	74.03	47.01	257	92	7	92	Gauss	IBM 3033	142	
Chevron	28.88	73.94	47.13	217	98	27	632	D4-Gauss	IBM 370/168	942	Multi-programming environment
D&S	29.11	74.97	47.11	315	158	7	290	Iter. D4	VAX 11/780	903	
Franlab	28.89	73.93	47.09	280	122	10	122	Gauss	VAX 11/780	1,947	
Gulf	29.29	73.49	47.63	230	37	2	94	D4-Gauss	IBM 3033	64.1	Point-centered grid
Harwell	28.89	73.96	47.09	232	44	3	161	Iter.	Cray-1S	15.7	Not vectorized
	28.89	73.96	47.09	232	44	3	161	Iter.	IBM 3033	54.3	
Intercomp	28.92	73.93	47.13	210	14	2	78	D4-Gauss	Cray-1S	4.0	
McCord-Lewis	28.68	74.12	46.98	257	180	3	360	Gauss	IBM 3033	228	
	28.68	74.12	46.98	257	180	3	360	Gauss	Prime 750	1,110	
Nolen	28.89	73.96	47.08	237	33	3	95	D4-Gauss	CDC 176	26.3	Automatic timesteps
	28.89	73.96	47.08	237	33	3	95	D4-Gauss	CDC 203	12.2	Automatic timesteps
	28.89	73.96	47.08	237	33	3	95	D4-Gauss	CDC 205	3.7	Automatic timesteps
	28.89	73.96	47.08	237	20	3	77	D4-Gauss	CDC 176	21.3	Specified timesteps
SSC	28.87	74.03	47.04	250	63	9	237	Gauss	Cray-1S	13.9	
Shell	28.76	74.08	46.94	222	118	13	231	D4-Gauss	Univac 1100/84	280	



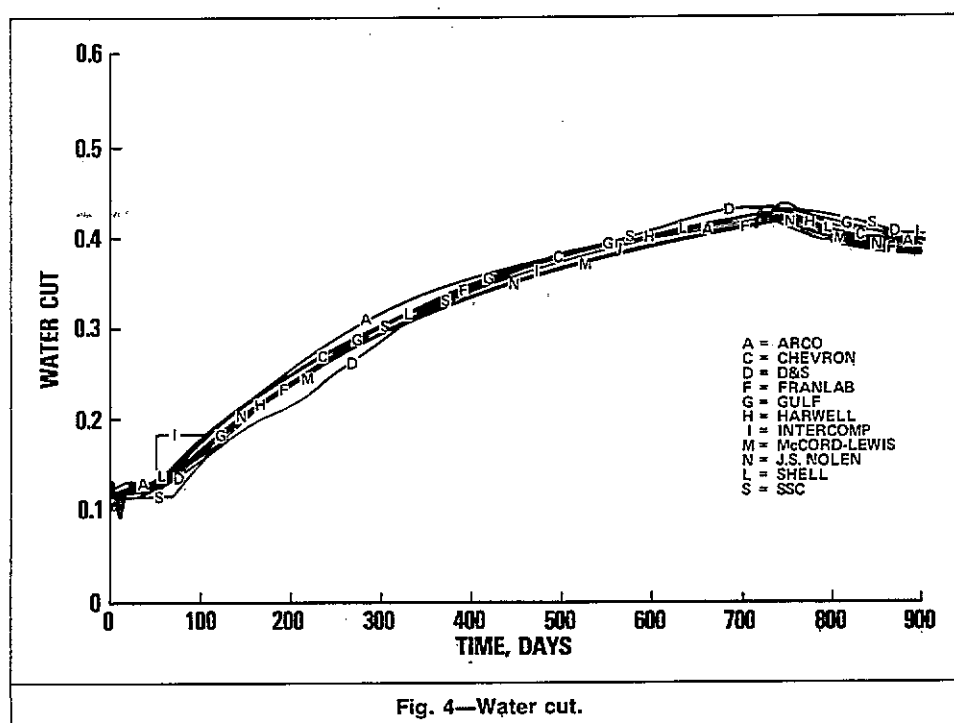
The finite-difference equations may be solved either iteratively or with D4 Gaussian elimination. A normalized variation of Stone's second method is used to calculate relative permeabilities; single-point upstream weighting is applied in the finite-difference equations.

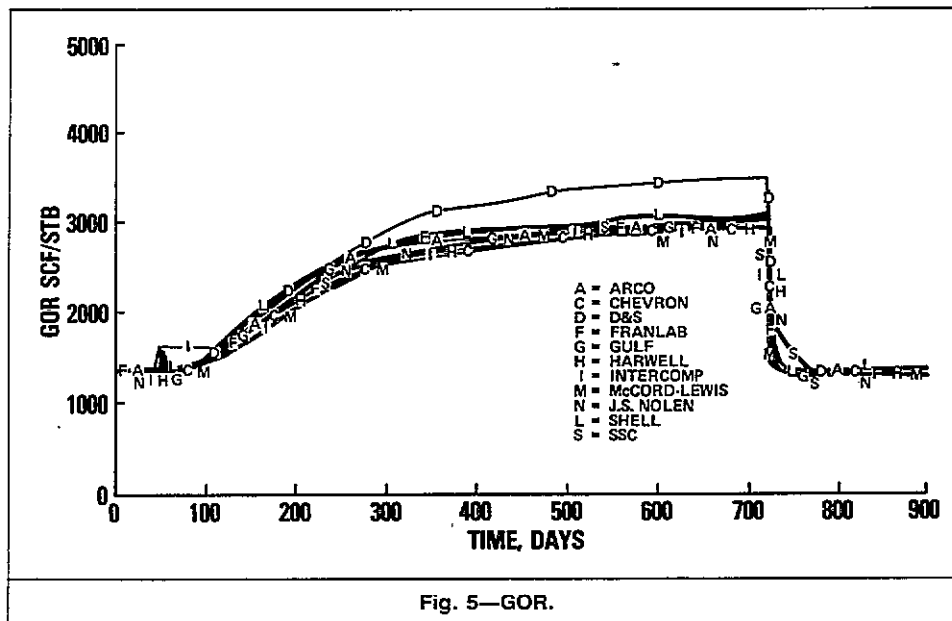
D4 Gaussian elimination was used to solve the test problem. Two solutions were submitted, one that used automatic timestep control and one that used specified timesteps. The objective of the run with specified timesteps was to solve the problem in the minimum number of timesteps that would not adversely affect the results. Results from the two runs were virtually identical.

**Scientific Software Corp.** Scientific Software Corp. (SSC) has developed a black-oil model that employs an adaptive implicit method (AIM).<sup>12</sup> This technique seeks to achieve an optimum with respect to stability, trunca-

tion error, and computer cost. Typically, during simulation only a small fraction of the total number of gridblocks experiences sufficiently large surges in pressure and/or saturation to justify implicit treatment. When it is needed, implicit treatment may not be required in all phases or for long periods of time. Moreover, those cells requiring implicit treatment will change as the simulation proceeds. Various degrees of implicitness are invoked regionally or individually cell by cell; i.e., the solution is advanced with adjacent cells having different degrees of implicitness. One can also override and operate in a fully implicit, partially implicit, or an IMPES mode.

The simulator is a general-purpose package offering 3D capability in both Cartesian and cylindrical coordinates. Variable bubblepoint problems are handled by variable substitution. Normal-order Gaussian elimination is used to solve the finite-difference equations. Relative permea-



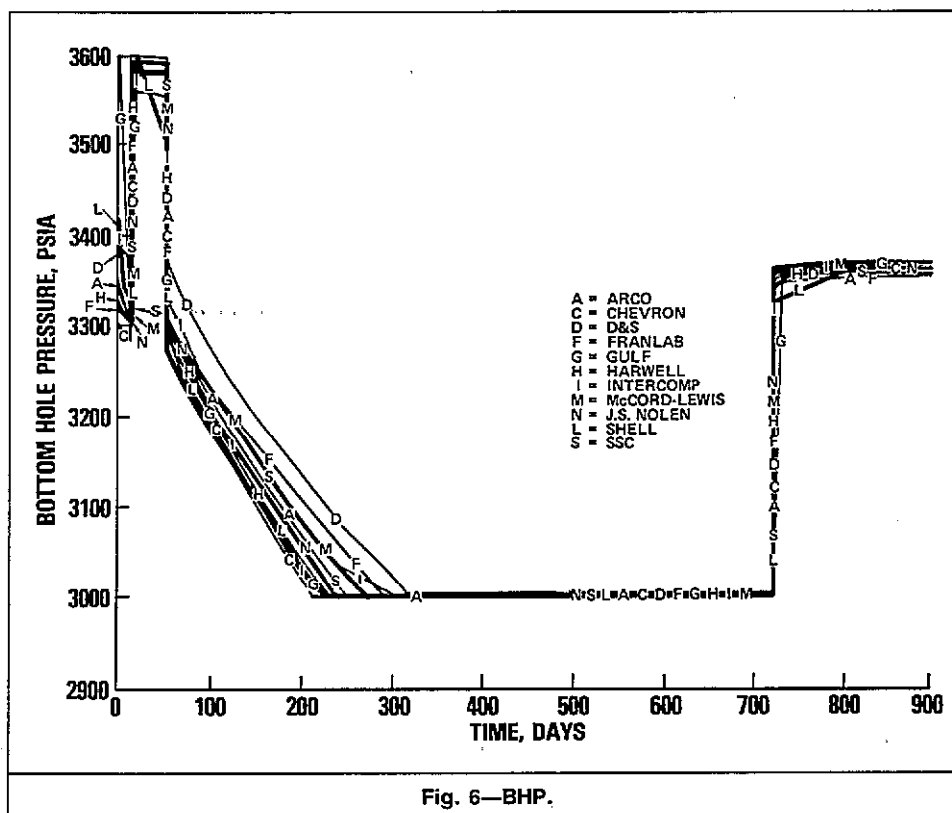


bilities are evaluated by the Dietrich-Bondor variation of Stone's second method. Single-point upstream weighting is used for relative permeability, and in addition, harmonic weighting may be applied to the total mobility,  $\lambda_T$ .<sup>13</sup>

**Shell Development Co.** The Shell isothermal reservoir simulation system<sup>14</sup> operates either in an IMPES or semi-implicit mode. The dependent variables, solved simultaneously in the implicit mode, are the oil-phase pressure, water-phase saturation, and oil-phase saturation. The three equations of mass conservation for the three pseudocomponents are discretized in a consistent manner. Relative

permeabilities and capillary pressure are assumed to be linear functions of the new saturation (semi-implicit). The equations for the wells are also treated in the same way, and the wellbore pressure or rate is solved simultaneously with the other dependent variables. The equations are written in residual form and are solved directly for the change per iteration in the dependent variables by a direct method with D4 numbering. Nonlinear terms are updated and the equations re-solved until the error in each equation reaches a prescribed level.

Timesteps are chosen automatically in a method previously described.<sup>14</sup> Failure to meet various criteria (e.g.,



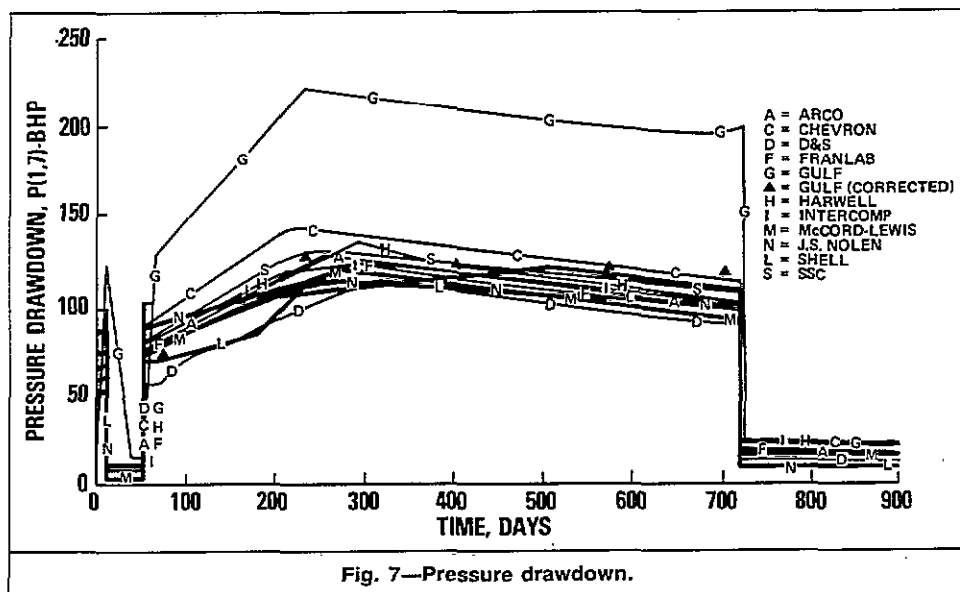


Fig. 7—Pressure drawdown.

nonconvergence or too large a saturation change) can cause a recalculation with a suitably smaller value for the timestep.

Moving pictures can be made from arrays that are stored for use as potential restart points.

### Statement of the Problem

A cross-sectional view of the reservoir is presented in Fig. 1, and the reservoir properties and stratification are detailed in Table 2. The reservoir is initially at capillary/gravity equilibrium with a pressure of 3,600 psia [24.8 MPa] at the gas/oil contact depth of 9,035 ft [2754 m]. The water/oil contact is located at a depth of 9,209 ft [2807 m]. The reference capillary pressure at each contact is 0 psi. The single production well at the center of the radial system is completed in Blocks 1,7 and 1,8. Other pertinent basic data are given in Table 3. Saturation functions and PVT properties are displayed in Tables 4 and 5. Water FVF and density in Table 5 were actually calculated from given formulas:

$$B_w = B_{wb} / [1 + C_w(p - p_b)]$$

and

$$\rho_w = \rho_{wb} [1 + C_w(p - p_b)],$$

where  $B_{wb} = 1.0142$  RB/STB [1.0142 res m<sup>3</sup>/stock-tank m<sup>3</sup>],  $\rho_{wb} = 62.14$  lbm/cu ft [995 kg/m<sup>3</sup>],  $p_b = 14.7$  psi [101 kPa], and  $C_w = 3 \times 10^{-6}$  psi<sup>-1</sup> [435  $\times 10^{-6}$  Pa<sup>-1</sup>].

Participants were asked to carry out computer calculations and report the results described below.

### Results To Be Reported

The results that were to be reported included the number of timesteps; CPU time and computer time (report for more than one computer, if possible); the total number of nonlinear updates (iterations on nonlinear terms); the total number of timestep cuts; the time when the well goes on decline (if ever); the initial fluids in place; and plots of initial gas and water saturation profiles vs. depth, oil production rate vs. time, water cut vs. time, GOR vs. time, BHP vs. time, and pressure drawdown [p(1,7)-BHP] vs. time.

### Results

Consensus initial gas and water saturation distributions are shown in Fig. 2. A comparison of results is given in Table 6 and Figs. 3 through 7.

Gulf employed a point-centered grid. All of their calculations are in good agreement with those of the other companies with the exception of the pressure drawdown curve (Fig. 7). Discrepancies in the latter can be explained by the fact that, in the point-centered grid, the radial position of the first interior calculation point is 2.0 ft [0.61 m], whereas in the block-centered framework the distance is 0.84 ft [0.26 m]. If one assumes, albeit somewhat inaccurately, the steady-state logarithmic variation of pressure with radial position, then the pressure drawdown, corrected to block-centered location, is given by

$$\Delta p_b = \Delta p_p \frac{\ln(r_b/r_w)}{\ln(r_p/r_w)},$$

where  $\Delta p$  is the pressure drawdown and subscripts  $b$  and  $p$  refer to block-centered and point-centered, respectively. For this test case,  $r_b = 0.84$  ft [0.26 m],  $r_p = 2.0$  ft [0.61 m], and  $r_w = 0.25$  ft [0.08 m], yielding  $\Delta p_b = 0.583 \Delta p_p$ . Selected values of  $\Delta p_b$  are plotted as closed triangles on Fig. 7 to show the agreement with the other block-centered values.

### Use as a Test Problem

During the course of designing the test problem, it was found that various changes in the input data could make the problem much more difficult to run. We list these here for potential use in checking new simulators.

1. The well  $kh$  is equal to the layer  $kh$ . If the well  $kh$  of the lower (tight) layer is made equal to or larger than that of the upper layer, the bottomhole flowing pressure (BHFP) will play a significant role in production allocation between layers.

2. The  $kv/kh$  ratio is 0.1. If it is set to 0.5, much more coning will occur. Thus the transients in saturations will be more significant.

3. If the higher production rate is doubled or tripled, pressure transients will be more significant.

4. If the BHFP limit is lowered and the rate is increased, more gridblocks will go through the bubblepoint. Then, when the rate is diminished, more of the reservoir will become undersaturated.

We had considered asking what was the approximate "mathematical" solution to the problem (as posed), as well as what was a reasonable "engineering" solution. This question, although of considerable interest, seemed to be difficult to formulate precisely. We solicit written remarks on this point, as well as comments on any other aspects of the problem or the individual solutions obtained.

## Nomenclature

- $B_g$  = gas FVF, Mcf/STB [res m<sup>3</sup>/stock-tank m<sup>3</sup>]  
 $B_o$  = oil FVF, RB/STB [res m<sup>3</sup>/stock-tank m<sup>3</sup>]  
 $B_w$  = water FVF, RB/STB [res m<sup>3</sup>/stock-tank m<sup>3</sup>]  
 $B_{wb}$  = water FVF at base pressure  $p_b$ , RB/STB [res m<sup>3</sup>/stock-tank m<sup>3</sup>]  
 $C_w$  = water compressibility, psi<sup>-1</sup> [kPa<sup>-1</sup>]  
 $kh$  = permeability/thickness product, md-ft [md·m]  
 $k_{rg}$  = gas relative permeability, dimensionless  
 $k_{rog}$  = oil relative permeability in gas/oil system, dimensionless  
 $k_{row}$  = oil relative permeability in water/oil system, dimensionless  
 $k_{rw}$  = water relative permeability, dimensionless  
 $k_v/k_h$  = vertical-to-horizontal permeability ratio  
 $k_x$  = absolute permeability in radial direction, md  
 $k_z$  = absolute permeability in vertical direction, md  
 $p$  = pressure, psia [kPa]  
 $p_b$  = base pressure, psia [kPa]  
 $p_o$  = oil pressure, psia [kPa]  
 $P_{cgo}$  = gas/oil capillary pressure, psi [kPa]  
 $P_{cow}$  = oil/water capillary pressure, psi [kPa]  
 $r_b$  = radial location of first block-centered calculation point, ft [m]  
 $r_p$  = radial location of first point-centered calculation point, ft [m]  
 $r_s$  = vaporized oil/gas ratio, STB/scf [stock-tank m<sup>3</sup>/std m<sup>3</sup>]  
 $r_w$  = wellbore radius, ft [m]  
 $R_s$  = solution GOR, scf/STB [std m<sup>3</sup>/stock-tank m<sup>3</sup>]  
 $S_g$  = gas saturation, %  
 $S_o$  = oil saturation, %  
 $S_w$  = water saturation, %  
 $\delta X$  = change in unknown  $X$   
 $\Delta p_b$  = pressure drawdown [p(1,7)-PBH] in block-centered grid, psi [kPa]  
 $\Delta p_p$  = pressure drawdown [p(1,7)-PBH] in point-centered grid, psi [kPa]  
 $\lambda_t$  = total mobility

$$\rho_w = \text{water density, lbm/cu ft [kg/m}^3\text{]}$$

$$\rho_{wb} = \text{water density at base pressure } p_b, \text{ lbm/cu ft [kg/m}^3\text{]}$$

## References

- Odeh, A.S.: "Comparison of Solutions to a Three-Dimensional Black-Oil Reservoir Simulation Problem," *J. Pet. Tech.* (Jan. 1981) 13-25.
- Price, H.S. and Coats, K.H.: "Direct Methods in Reservoir Simulation," *Soc. Pet. Eng. J.* (June 1974) 295-308; *Trans.*, AIME, 257.
- Stone, H.L.: "Probability Model for Estimating Three-Phase Relative Permeability," *J. Pet. Tech.* (Feb. 1970), 214-18; *Trans.*, AIME, 249.
- Stone, H.L.: "Estimation of Three-Phase Relative Permeability and Residual Oil Data," paper presented at the 1973 Annual Technical Meeting of CIM, Edmonton, Canada, May 8-12.
- Tan, T.B.S. and Letkeman, J.P.: "Application of D4 Ordering and Minimization in an Effective Partial Matrix Inverse Iterative Method," paper SPE 10493 presented at the 1982 SPE Symposium on Reservoir Simulation, New Orleans, Feb. 1-3.
- Sonier, F., Besset, P., and Ombret, O.: "A Numerical Model of Multiphase Flow Around a Well," *Soc. Pet. Eng. J.* (Dec. 1973) 311-20.
- Dietrich, J.K. and Bondor, P.L.: "Three-Phase Oil Relative Permeability Models," paper SPE 6044 presented at the 1976 SPE Annual Technical Conference and Exhibition, New Orleans, Oct. 3-6.
- Cheshire, I.M., Appleyard, J.R., and Banks, D.: "An Efficient Fully Implicit Simulator," paper 179 presented at the 1980 European Offshore Petroleum Conference, London, Oct. 21-24.
- Patton, J.T., Coats, K.H., and Spence, K.: "Carbon Dioxide Well Stimulation: Part 1—A Parametric Study," *J. Pet. Tech.* (Aug. 1982) 1798-1804.
- Nolen, J.S. and Stanat, P.L.: "Reservoir Simulation on Vector Processing Computers," paper SPE 9644 presented at the 1981 SPE Middle East Technical Conference, Bahrain, March 9-12.
- Stanat, P.L. and Nolen, J.S.: "Performance Comparisons for Reservoir Simulation Problems on Three Supercomputers," paper SPE 10640 presented at the 1982 SPE Symposium on Reservoir Simulation, New Orleans, Feb. 1-3.
- Thomas, G.W. and Thurnau, D.H.: "The Mathematical Basis of the Adaptive Implicit Method," paper SPE 10495 presented at the 1982 SPE Symposium on Reservoir Simulation, New Orleans, Feb. 1-3.
- Vinsome, P.K.W. and Au, A.D.K.: "One Approach to the Grid Orientation Problem in Reservoir Simulation," paper SPE 8247 presented at the 1979 SPE Annual Technical Conference and Exhibition, Las Vegas, Sept. 23-26.
- Chappellear, J.E. and Rogers, W.: "Some Practical Considerations in the Construction of a Semi-Implicit Simulator," *Soc. Pet. Eng. J.* (June 1974) 216-20.

## SI Metric Conversion Factors

bbl	× 1.589 873	E-01 = m <sup>3</sup>
cp	× 1.0*	E-03 = Pa·s
cu ft	× 2.831 685	E-02 = m <sup>3</sup>
ft	× 3.048*	E-01 = m
lbm/cu ft	× 1.601 846	E+01 = kg/m <sup>3</sup>
md-ft	× 3.280 839	E+00 = md·m
psi	× 6.894 757	E+00 = kPa
psi <sup>-1</sup>	× 1.450 377	E-01 = kPa <sup>-1</sup>

\*Conversion factor is exact.

JPT

Original manuscript received in the Society of Petroleum Engineers office Feb. 15, 1982. Paper accepted for publication March 22, 1983. Revised manuscript received Dec. 2, 1985. Paper (SPE 10489) first presented at the 1982 SPE Symposium on Reservoir Simulation held in New Orleans, Jan. 31-Feb. 3.

TABLE 5 - PVT PROPERTIES

Pressure (psia)	Saturated Oil				Water			Gas		
	$B_o$ (RB/STB)	Density (lbm/cu ft)	Visc. (cp)	Solution GOR (scf/STB)	$B_w$ (RB/STB)	Density (lbm/cu ft)	Visc. (cp)	$B_g$ (mcf/STB)	Density (lbm/cu ft)	Visc. (cp)
400	1.0120	46.497	1.17	165	1.01303	62.212	0.96	5.90	2.119	0.0130
800	1.0255	48.100	1.14	335	1.01182	62.286	0.96	2.95	4.238	0.0135
1200	1.0380	49.372	1.11	500	1.01061	62.360	0.96	1.96	6.379	0.0140
1600	1.0510	50.726	1.08	665	1.00940	62.436	0.96	1.47	8.506	0.0145
2000	1.0630	52.072	1.06	828	1.00820	62.510	0.96	1.18	10.596	0.0150
2400	1.0750	53.318	1.03	985	1.00700	62.585	0.96	0.98	12.758	0.0155
2800	1.0870	54.399	1.00	1130	1.00580	62.659	0.96	0.84	14.885	0.0160
3200	1.0985	55.424	0.98	1270	1.00460	62.734	0.96	0.74	16.896	0.0165
3600	1.1100	56.203	0.95	1390	1.00341	62.808	0.96	0.65	19.236	0.0170
4000	1.1200	56.930	0.94	1500	1.00222	62.883	0.96	0.59	21.192	0.0175
4400	1.1300	57.534	0.92	1600	1.00103	62.958	0.96	0.54	23.154	0.0180
4800	1.1400	57.864	0.91	1676	0.99985	63.032	0.96	0.49	25.517	0.0185
5200	1.1480	58.267	0.90	1750	0.99866	63.107	0.96	0.45	27.785	0.0190
5600	1.1550	58.564	0.89	1810	0.99749	63.181	0.96	0.42	29.769	0.0195

TABLE 6 - COMPARISON OF CALCULATED RESULTS

Company	Initial Fluids in Place			Time on Decline, Days	Timesteps	Timestep Cuts	Non-linear Updates	Matrix Solution	Computer	CPU Time, Seconds	Comments
	Oil, 10 <sup>6</sup> STB	Water, 10 <sup>6</sup> STB	Gas, 10 <sup>6</sup> SCF								
Arco	28.80	74.03	47.01	257	92	7	92	Gauss	IBM 3033	142	
Chevron	28.88	73.94	47.13	217	98	27	632	D4-Gauss	IBM 370/168	942	Multiprogramming Environment
D & S	29.11	74.97	47.11	315	158	7	290	Iter. D4	VAX 11/780	903	
Franlab	28.89	73.93	47.09	280	122	10	122	Gauss	VAX 11/780	1947	
Gulf	28.90	73.92	47.08	218	38	2	178	D4-Gauss	IBM 3033	397	Block-centered grid
	29.29	73.49	47.63	235	31	6	176	"	"	572	Point-centered grid
	"	"	"	"	"	"	"	"	IBM 370/168	1039	"
Harwell	28.89	73.96	47.09	232	44	3	161	Iter.	Cray-1S	15.7	Not vectorized
	"	"	"	"	"	"	"	"	IBM 3033	54.3	
Intercomp	28.92	73.93	47.13	57	14	2	69	D4-Gauss	Cray-1S	3.6	
McCord-Lewis	28.68	74.12	46.98	257	180	3	360	Gauss	IBM 3033	228	
	"	"	"	"	"	"	"	"	Prime 750	1110	
Nolen	28.89	73.96	47.08	237	33	3	95	D4-Gauss	CDC 176	26.3	Automatic timesteps
	"	"	"	"	"	"	"	"	CDC 203	12.2	"
	"	"	"	"	20	"	77	"	CDC 205	3.7	"
									CDC 176	21.3	Specified timesteps
SSC	28.87	74.03	47.04	250	63	9	237	Gauss	Cray-1S	13.9	
Shell	28.76	74.08	46.94	222	118	13	231	D4-Gauss	Univac 1100/84	280	

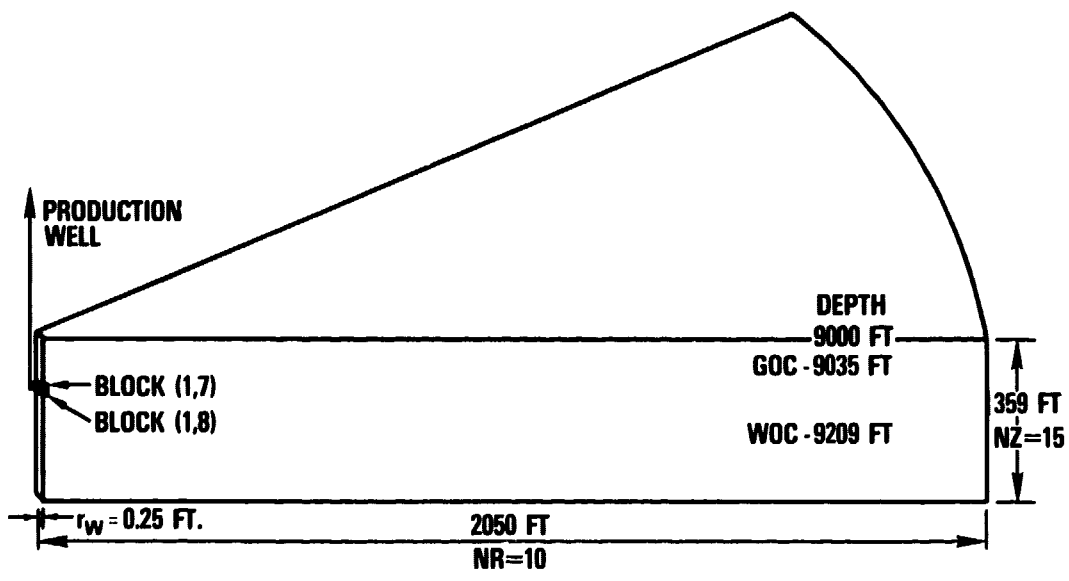


FIGURE 1  
RESERVOIR MODEL

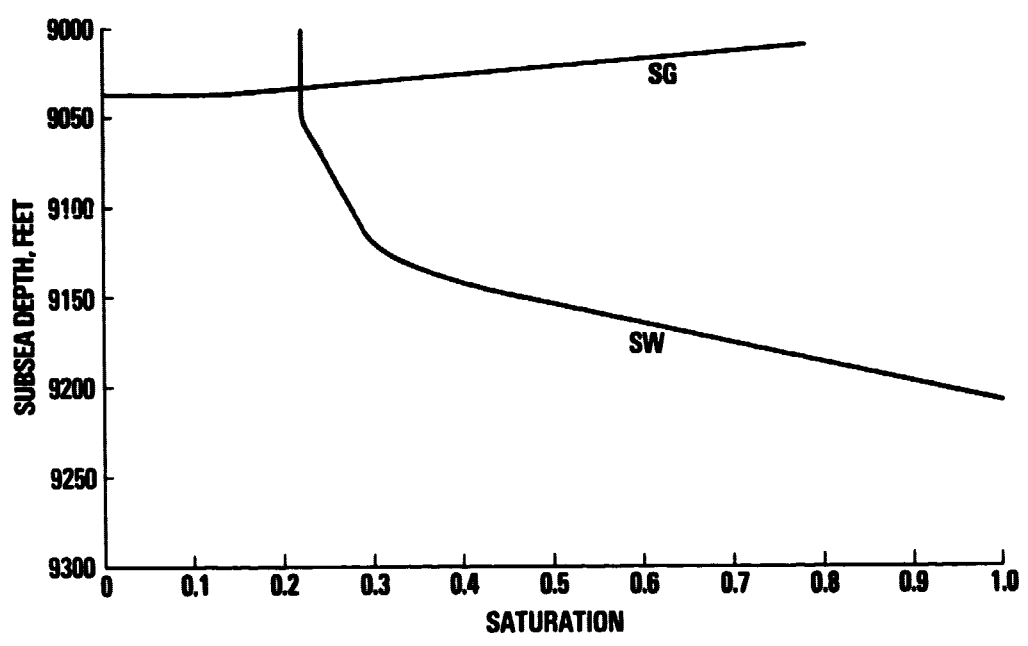
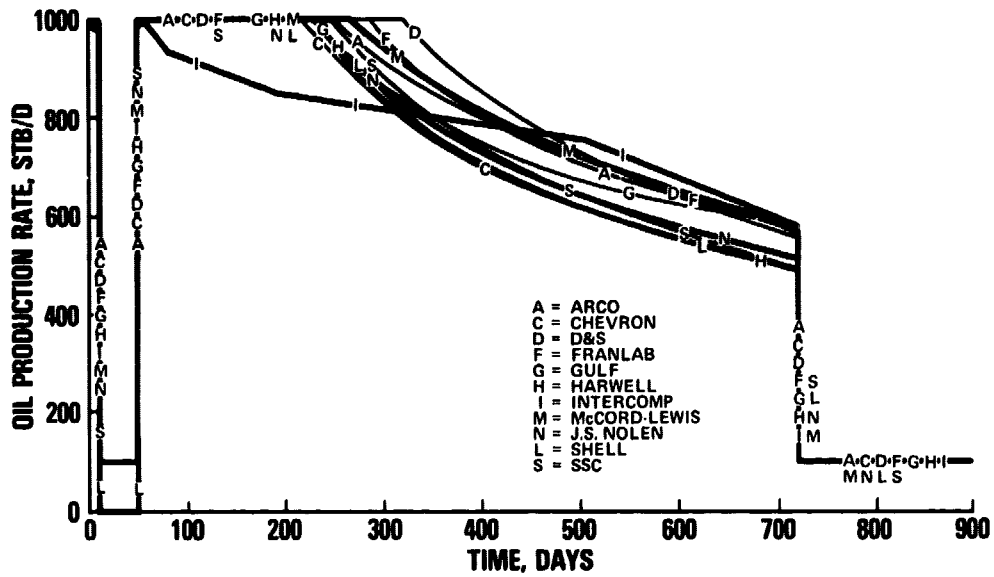
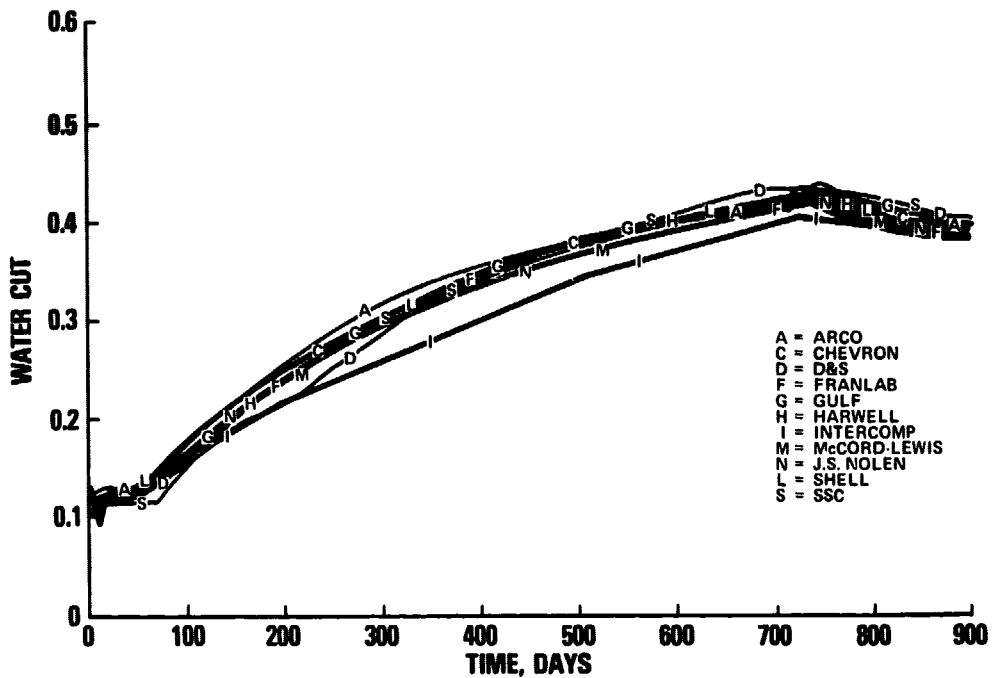


FIGURE 2  
INITIAL SATURATION DISTRIBUTION



**FIGURE 3  
OIL PRODUCTION RATE**



**FIGURE 4  
WATER CUT**

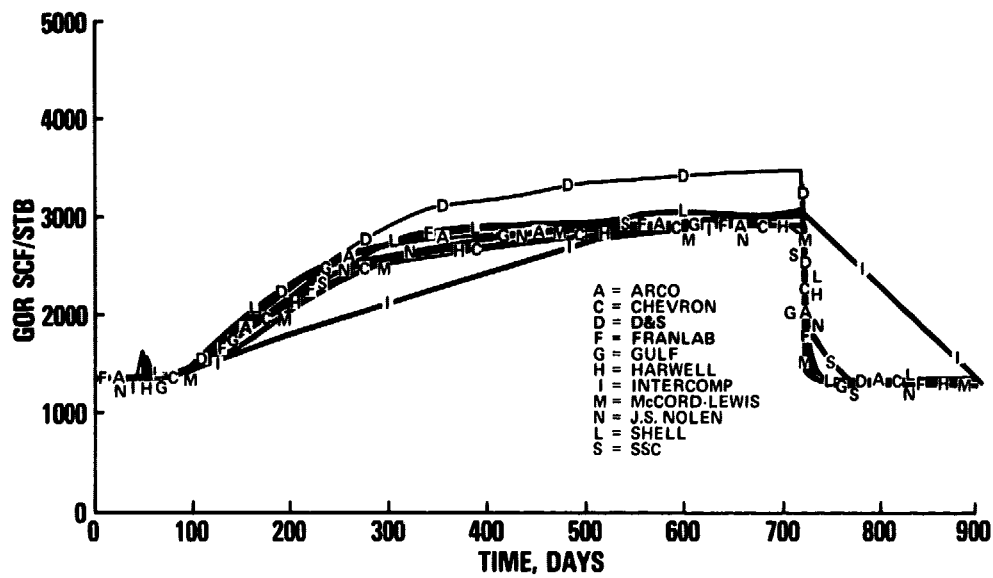


FIGURE 5  
GAS OIL RATIO

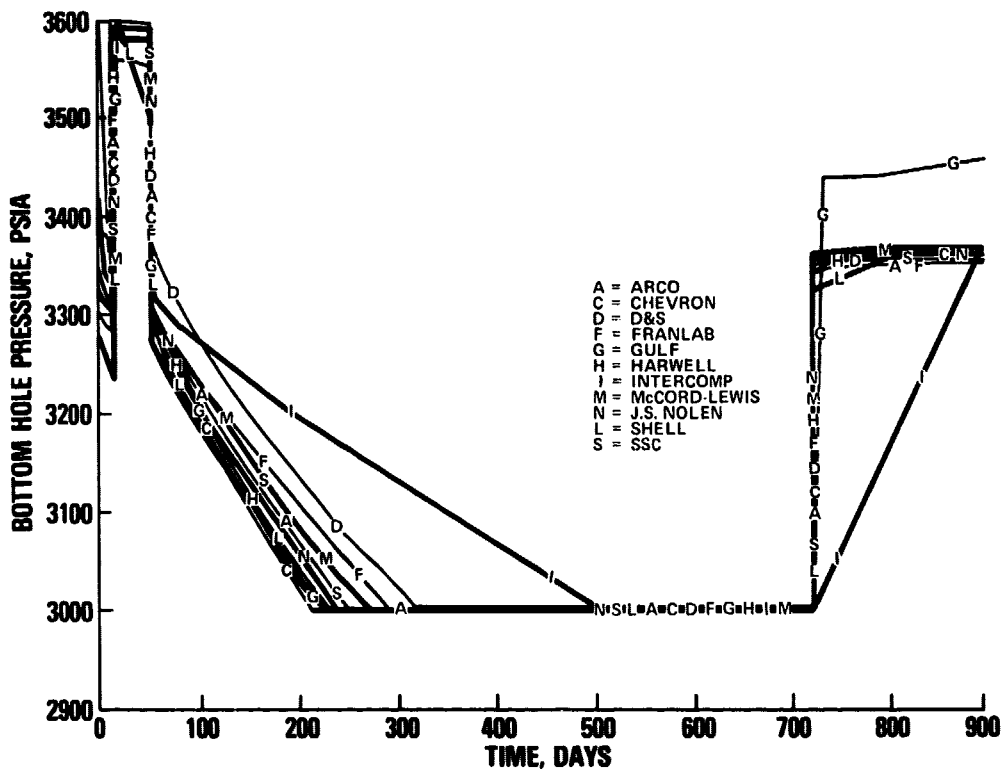
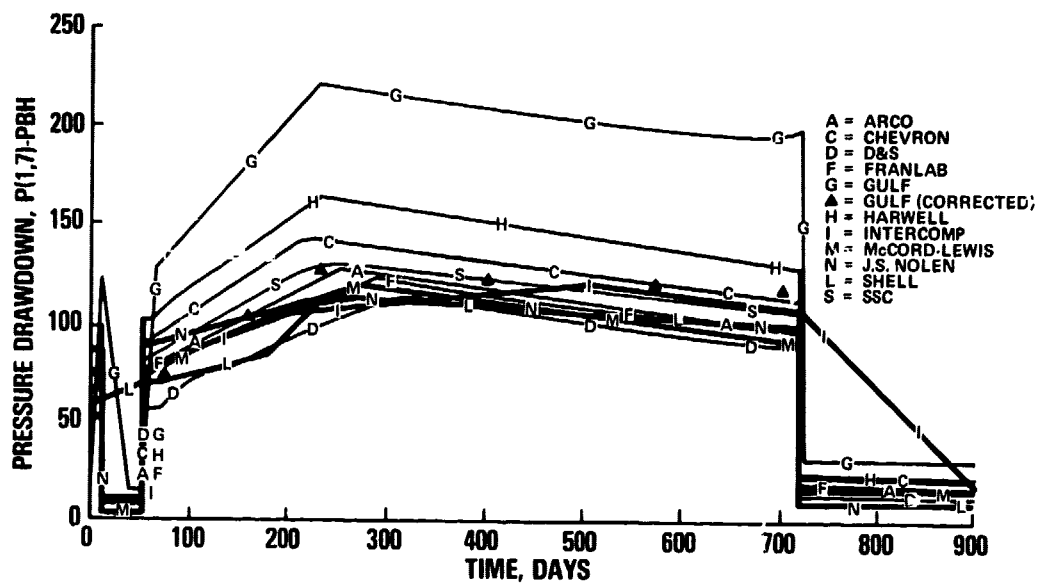


FIGURE 6  
BOTTOM HOLE PRESSURE



**FIGURE 7**  
**PRESSURE DRAWDOWN**